MECHANICAL PROPERTIES AND IMPULSIVE RESPONSE OF 3D-KAGOME TRUSS CORE SANDWICH PANEL

Li MA, Hua-Yong ZHENG, Lin-Zhi WU
Center for Composite Materials, Harbin Institute of Technology

Keywords: *truss core; Kagome; sandwich structure; effective property; impulsive response*

Abstract

Sandwich structure with Kagome truss core is brought forward in recent years. The effective performance calculation model of 3D-Kagome truss core is established in this paper firstly. Then the analytical model of 3D-Kagome truss core panels subjected to idealized impulsive loads is carried out. The truss core with a mass of periodic unit cells is identified as solid plate. The equivalent constitutive model for Kagome core is employed and the equivalent strength and stiffness of the core is obtained. The transient dynamics analysis software MSC. Dytran is adopted to simulate the response of 3D-Kagome truss core sandwich panels subjected to idealized impulsive loads. The response of the displacement, velocity and effective stress in the whole time history are obtained. The variations of maximum deflections of the plate with the relative density and the thickness of the core and impulsive loads are investigated. Thus, the optimum design program of the structure for impulse resistance is given.

1 Introduction

The multifunctional properties of cellular solids have generated great interest for their application in ultra-light structures. The properties that appear most attractive are those that govern the use of cellular solids as cores for panels and shells having lower weight than competing materials, and potentially superior heat dissipation, vibration control and energy dissipation characteristics [1~4]. Commercially available cellular solids and foams have random microstructures and their properties have been thoroughly documented (see for example Refs. [1, 3]). An interesting research trend in cellular materials consists of the study and the application of deterministic periodic architectures, whose topology can be designed and tailored for the considered component to achieve performances greatly superior than those demonstrated by their stochastic analogues [3]. The scalable geometry of deterministic periodic architectures, whereby the structural properties depend on the actual size of the unit cells, allows for their application to both small-scale and large-scale structural systems. Examples of applications of deterministic periodic cellular architectures include the lattice material and prismatic core concepts [2, 5]. Both configurations have been employed and studied in the past as alternative core configurations for sandwich structures with superior structural characteristics and potential multifunctional capabilities. For example, the application of the lattice material concept has lead to the design of truss core sandwich constructions, whose optimized structural performance has proven to be competitive with traditional sandwich honeycomb and stiffened structures [5].

Xue and Hutchinson [6, 7] investigated the dynamic responses of clamped circular sandwich plate with a tetragonal truss, pyramidal truss, square honeycomb core subjected to identical initial momentum impulses.

The performance of 3D-Kagome topology has been explored by the finite element simulations presented by Hyun et al. [8] and has been measured by Wang et al. [9]. The results indicate advantages over other cores, primarily because of superior isotropy and greater resistance to softening modes (such as plastic buckling).

The dynamic responses of clamped rectangle Kagome truss core sandwich plate subject to uniformly distributed impulsive loads applied to one face sheet of the sandwich is studied in the present paper.

The study is conducted within the framework of dynamic, finite strain plasticity for an elastic-perfectly plastic solid with no rate dependence. Computations are preformed using the explicit time integration version of the commercially available code MSC.Dytran [10]. The simulations capture limits to deformation due to necking localization, however, no consideration will be made in this study of limits due to fracture. The focus will be on the comparison between sandwich plates and solid plates assuming each is able to withstand fracture. If the plates are constructed from a material with good ductility, this is tantamount to comparing them over the range of impulsive for which deformations are comparable.

For each impulse level, the maximum deflection is compared to that of a solid plate of the same mass. The core is envisioned to be a Kagome truss structure and is modeled by a continuum plasticity relation developed previously for metal foam cores having a specific crushing strength. This crushing strength is matched to the corresponding strength of the truss core. The role of the strength of the core is studied via variations in its relative density, and some insight into an optimal design of the sandwich structure is obtained.

2 Formulation of the problem

A rectangle Kagome truss core sandwich plate of length $2L$ and width $2W$ that are clamped along their edges are considered, as depicted schematically in Fig.1. The plate has two identical face sheets of thickness, H_f , bonded to a 3D-Kagome truss structure core of thickness, H_c. The face sheets and the truss elements are made from the same material with density, ρ , Young's modulus, E , Poisson's ratio, υ .

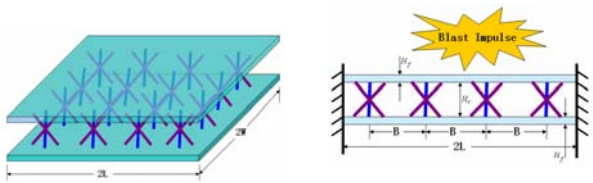

Fig.1. A schematic of a edge-clamped Kagome truss core sandwich panel subjected to impulsive loading

Explosives create a pressure wave with a triangular-like profile, known as a "blast" [6] as shown in Fig.2. The blast exerts an impulse, I , on the plate, which is equal to the integral of the total force over time

$$I = \int p(t)dAdt = A\int p(t)dt \tag{1}$$

where A is the area of the plate, then the impulse per area can be written as

$$\hat{I} = \frac{I}{A} = \int p(t)dt \tag{2}$$

Here, we assumed that the pressure caused by impulsion is applied to the top face sheet of the sandwich uniformly, thus the pressure P dependent only on the time t as shown in the expression (1).

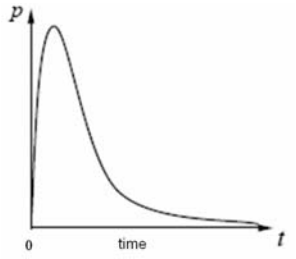

Fig.2. A schematic diagram of a pressure-time pulse

3 Continuum constitutive model for 3D-Kagome truss core

No attempt has been made to carry out calculations for the sandwich plate using full meshing of individual truss elements. Although such calculations might be feasible for a limited number of cases, they would be extremely large and would not permit an exploration of trends, which is the main goal here. Instead, a more practical approach is to model the core as a solid whose effective properties mimic those of the Kagome truss core between face sheets. At the present work, a constitutive model for the Kagome truss core has been developed. Here, a constitutive model is adopted that was developed for metal foams by Deshpande and Fleck [11]. The model permits one to set the crushing strength of the core to match values appropriate to the Kagome truss. Moreover, the model represents a material with high porosity similar to that of the truss core. The model is dilatational plasticity relation that employs an isotropic yield surface specified by

$$\hat{\sigma} = \sigma_Y^c \tag{3}$$

where $\hat{\sigma}$ is an equivalent stress, defined by

$$\hat{\sigma}^2 = \frac{1}{1+(\alpha/3)^2}\left[\sigma_e^2 + \alpha^2\sigma_m^2\right] \tag{4}$$

Here, $\sigma_e = \sqrt{3s_{ij}s_{ij}/2}$ is the conventional effective stress with s_{ij} as the stress deviator, and

$\sigma_m = \sigma_{kk}/3$ as the mean stress. The compressive yield stress, σ_Y^c, is a prescribed function of the equivalent plastic strain using date taken under uniaxial compression. Normality of the plastic flow is assumed. For metal foams, the parameter α is usually chosen to produce a specific plastic Poisson's ratio $\upsilon_p = -\dot{\varepsilon}_{22}^p / \dot{\varepsilon}_{11}^p$ corresponding to uniaxial compression in the one-direction [1], i.e.,

$$\alpha = 3\left(\frac{1/2-\upsilon_p}{1+\upsilon_p}\right)^{1/2} \text{ or } \upsilon_p = \frac{1/2-(\alpha/3)^2}{1+(\alpha/3)^2} \quad (5)$$

The flow stress, τ_Y^c, in shear is related to that in compression at the same equivalent plastic by

$$\tau_Y^c = \left[\frac{1+(\alpha/3)^2}{3}\right]^{1/2} \quad (6)$$

4 Effective mechanical properties of a 3D-Kagome truss core

A Kagome truss core element is configured as shown in Fig.3. Different from the tetrahedron or pyramidal truss core, the strut of the Kagome truss core between the unit cell does not be joined each other. The properties of all members of the core are identical with length L_c and a solid circular cross-section of radius R_c. The angle ω can be described as $\sin\omega = H_c/2L_c$ and the distance between each element is B as shown in Fig.1 and Fig.3. The relative density of the core (defined by the density of the core divided by the density of the solid from which it is made) is

$$\bar{\rho}_c = \frac{\rho_c}{\rho} = \frac{6\pi L_c}{H_c}\left(\frac{R_c}{B}\right)^2 = \frac{3\pi}{\sin\omega}\left(\frac{R_c}{B}\right)^2 \quad (7)$$

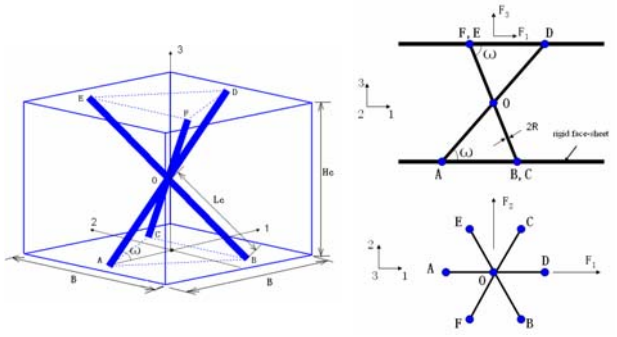

Fig.3. A schematic of the unit cell structure of 3D-Kagome truss core

The normal modulus E_{33} is deduced by applying the load F_3 to the top face sheet of a representative Kagome unite cell, as defined in Fig.3, and by calculating the resulting normal displacement of the two face-sheets. Consequently, we obtain

$$\frac{E_{33}}{E} = 3\pi\sin^3\omega\frac{R_c^2}{B^2} = \bar{\rho}_c\sin^4\omega \quad (8)$$

As shown in Fig.3, triangular symmetry implies transverse isotropy of elastic properties, such that the transverse shear modulus of the core is independent of orientation within the 1-2 plane, giving $G_{13} = G_{23}$. The shear modulus G_{13} is deduced by applying the load F_1 to the top face sheet of a representative Kagome unite cell and by determining the work conjugate nodal displacement, to get

$$\frac{G_{13}}{E} = \frac{3\pi}{2}\sin\omega\cos^2\omega\frac{R_c^2}{B^2} = \frac{1}{8}\bar{\rho}_c\sin^2 2\omega \quad (9)$$

Now consider the strength of the Kagome truss core. The normal strength σ_{33} is associated with the simultaneous yield of all six bar, and is given by

$$\frac{\sigma_{33}}{\sigma_Y} = 3\pi\sin\omega\frac{R_c^2}{B^2} = \bar{\rho}_c\sin^2\omega \quad (10)$$

For both tensile and compressive loading, the transverse shear strength is specified in term of the magnitude of shear strength τ and its direction ψ with respect to the x_1-axis, as defined in Fig.1.

$$\sigma_{13} = \tau\cos\psi,\ \sigma_{23} = \tau\sin\psi,\ \sigma_{33} = 0 \quad (11)$$

Equilibrium dictates the relation between the force F_1, F_2 and the macroscopic shear stress τ, such that

$$F_1 = B^2\sigma_{13},\ F_2 = B^2\sigma_{23},\ F_3 = 0 \quad (12)$$

The Kagome truss core has the property that the initial yield surface and limit yield surface coincide for struts made from an elastic ideally plastic solid. On assuming that the single bar OA or OD tension attains the yield value $N_{OA/OD} = \pi R_c^2\sigma_Y$, the magnitude τ of the in-plane shear strength depends upon the orientation of in-plane loading according to

$$\frac{\tau}{\sigma_Y} = \frac{\bar{\rho}_c}{4}\frac{\sin 2\omega}{\cos\psi} = \frac{3\pi}{2\cos\psi}\left(\frac{R_c}{B}\right)^2\cos\omega \quad (13)$$

for $|\psi| \le \pi/6$. If instead, it is assumed that the single bar OC or OF tension attains the compressive yield value $N_{OC/OF} = -\pi R_c^2\sigma_Y$, then the macroscopic shear strength is

$$\frac{\tau}{\sigma_Y} = \frac{\bar{\rho}_c}{4}\frac{\sin 2\omega}{\cos(\psi-\pi/3)} = \frac{3\pi}{2\cos(\psi-\pi/3)}\left(\frac{R_c}{B}\right)^2\cos\omega \quad (14)$$

for $\pi/6 < \psi < \pi/2$. The solution for τ is periodic in ψ, with a period of $2\pi/3$, and reflects the symmetry of the structure. Each plane of the yield surface corresponds to a single strut attaining tensile or compressive yield, as summarized in Fig.4.

The compressive strength σ_{33} and the transverse shear strength τ are degraded when the strut bucking stress σ_c, as given by

$$\sigma_c = \frac{k^2 \pi^2 E_t R_c^2}{L_c^2} \tag{15}$$

is less than them material yield strength σ_Y; then, the expression (4) still pertains, but with the factor σ_Y replaced by σ_c. Similarly, the segments of the shear yield surface $\tau(\psi)$ which are associated with compressive yield of one of the struts are similarly reduced in magnitude: the relations (7) and (8) hold, but with σ_Y replaced by σ_c, as shown diagrammatically in Fig.4.

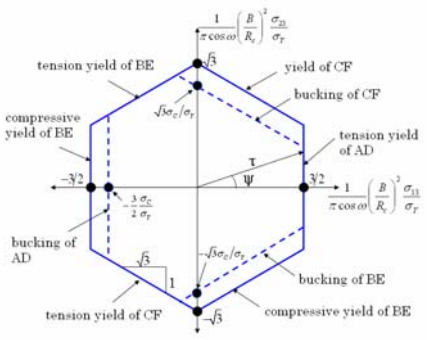

Fig.4. Yield and bucking collapse surface in transverse shear for Kagome core

At the present study, we considered the case of $\psi = 0$, namely, the shear strength of equivalent unit cell, τ_Y^c, can be written as

$$\frac{\tau_Y^c}{\sigma_Y} = \frac{3\pi}{2}\left(\frac{R_c}{B}\right)^2 \cos\omega = \frac{\overline{\rho}_c}{4}\sin 2\omega \tag{16}$$

5 Numerical model for finite element calculation

The structural response of the sandwich plate is split into three sequential steps [6, 12]: stage I is the one-dimensional fluid-structure interaction problem during the blast loading event, and results in a uniform velocity of the outer face sheet; during stage II the core crushes and the velocities of the faces and core become equalized by momentum sharing; stage III is the retardation phase over which the plate is brought to rest by plastic bending and stretching. Here we ignored the fluid-structure interaction, thus the impulse $\hat{I}$ can be imposed as uniform initial velocity $V_f = \hat{I}/\rho H_f$ prescribed throughout the top face sheet, then crushes the core and cause a velocity of whole sandwich plate.

The maximum deflection at the center of the plate can be expressed in functional form in term of dimensionless combinations as

$$\frac{\delta_{\max}}{L} = f\left[\frac{\hat{I}}{\overline{M}\sqrt{\sigma_Y/\rho}}, \frac{\overline{M}}{\rho L}, \frac{H_c}{L}, \rho_c, \frac{W}{L}\right] \tag{17}$$

Where, $\hat{I}$ is the impulse per area and $\overline{M}$ is the mass per area. It can be obtained from the

$$\frac{\overline{M}}{\rho L} = \frac{2H_f + \overline{\rho}_c H_c}{L} = \frac{H_s}{L} \tag{18}$$

where, H_s is the thickness of the solid plate which has same length and width and mass than the sandwich plate. Here, we assumed $\overline{M}/\rho L = 0.03$.

For convenience, we considered foursquare plate problem in the present study, i.e. $W/L = 1$. Let $\sin\omega = H_c/2L_c = \sqrt{2/3}$, so that $\overline{\rho}_c = 3\sqrt{6}\pi R_c^2/2B^2$, $E_c = 4\overline{\rho}_c E/9$, $\sigma_Y^c = 2\overline{\rho}_c\sigma_Y/3$ and $\tau_Y^c = \overline{\rho}_c\sigma_Y/3\sqrt{2} = \sigma_Y/2\sqrt{2}$. And in the constitutive model, we have taken $\alpha = 3/\sqrt{3}$ which, by (5) given $\upsilon_p = 0$. This choice corresponds to metal foams with a relative density typically in the range of 5-10% [3]. The choice $\upsilon_p = 0$ for modeling the Kagome core is motivated by the fact that its compressive behavior normal to the faces is essentially independent of deformations parallel to the faces.

Finite element calculations have been performed simulating the dynamic response of the plate using the commercial code MSC.Dytran [10]. In the calculations carried out below both the face sheets and the truss members are made from a moderately high strength steel with $\rho = 8000 kg/m^3$, $\sigma_Y = 500 MPa$, $E = 200 GPa$ and $\upsilon = 0.3$. The relative density of the regular Kagome core is given by (7). The compressive yields tress of the continuum constitutive model is given by (17), and $\alpha = 3/\sqrt{2}$ in (13). The elastic properties of the core are modeled as isotropic with Young's modulus (18) and Poisson's ratio, $\upsilon_c = 0$.

8-node hexahedron elements with reduced integration are used in the calculations. A uniform mesh is generated such that there are 5 and 15

divisions through the thickness of the face sheets and the core, respectively, but 80 divisions along the length and width for the whole plate. Additional studies showed that refined meshes with more elements did not appreciably improve the accuracy of numerical results. For the specific model, the numerical error for the maximum deflection based on the present meshing is believed to be less than 1%.

6 Impulsive response of 3D-Kagome truss core sandwich panel

Fig.5 presents the normalized maximum deflection $\delta_{\max}/L$ attained at the center of each face sheet as a function of the relative core density, $\overline{\rho}_c$, with $\hat{I}\sqrt{\rho/\sigma_Y}/\overline{M}=0.15$ and $H_c/L_c=0.1$ for impulses applied uniformly to the top face sheet. It can be found from the figure 5 that the top face sheet deflects more than the bottom sheet due to compaction of the core. The smallest maximum deflection occurs for a relative core density $\overline{\rho}_c\approx 0.1$. At lower core densities and, therefore, higher face sheet mass, the core undergoes so much compaction that it is not able to maintain the spacing of the face sheets such that the sandwich effect is eroded. At core densities above $\overline{\rho}_c\approx 0.1$, core mass is added at the expense of face sheet mass, rendering the faces too weak to be effective.

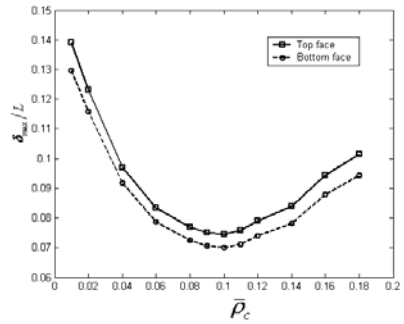

Fig.5 The normalized maximum deflection of the top and bottom face sheets of sandwich panels versus the relative density of the core

From the expression of relative density (7), the ratio of radius of the strut against the distance of the unit cell will be $R_c/B=0.093$, if let $B/L_c=1.5$, the ratio of the length of the strut of the corresponding Kagome truss core against its diameter will be $L_c/2R_c=3.6$. It can easily observed that the geometry of the strut at this state is appropriate and will yield primarily. In the other word, when the relative density is known, we can adjust the ratio of B/L_c to control the damage mode of the truss core structure by change the distance of the unit cell B.

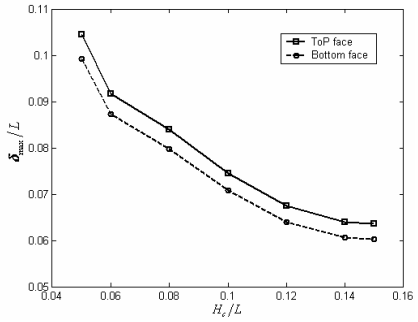

Fig.6 The normalized maximum deflection of the top and bottom face sheets of sandwich panels versus the relative thickness of the core

Let $\hat{I}\sqrt{\rho/\sigma_Y}/\overline{M}=0.15$, $\overline{\rho}_c=0.1$. From Eq. (18), it can be obtained, $2H_f/L+0.1H_c/L=0.03$, consider real deflection of the sandwich, the ratio of the thickness of the surface sheet against truss core should be chosen a adaptive value, $0.05\le H_f/H_c\le 0.25$ and $0.05\le H_c/L\le 0.15$. Fig.6 presents the normalized maximum deflection $\delta_{\max}/L$ of the top and bottom face sheet of the sandwich plate as a function of the normalized core height H_c/L. From the figure, with the increase of the H_c/L, the maximum deflection will decrease. This phenomena implies that with the increase of the proportion of the core, the stiffness and the capability for impulsion resist of the structure will increase.

Change the values of the impulse per area $\hat{I}$, we can compare the impulsion resist capability of the Kagome truss core sandwich plate and solid plate which has the same mass. When the impulse $\hat{I}$ applied to the solid plate, the plate attained the uniform velocity, $\overline{M}=\rho H_s$ and $V_0=\hat{I}/\rho H_s$. However, when the impulse $\hat{I}$ applied to the Kagome truss core sandwich plate, only top face sheet of the sandwich plate attained the uniform velocity, $\overline{M}=\rho H_f$ and $V_0=\hat{I}/\rho H_f$. Let the thickness of the solid plate is $H_s/L=0.03$, relative density of the Kagome core is $\overline{\rho}_c=0.1$, the

thickness of the Kagome core is $H_c/L=0.1$, the applied impulse is $1.2\le\hat{I}\le 15KN\cdot s/m^2$, normalized impulse $\hat{I}\sqrt{\rho/\sigma_Y}/\overline{M}$ variation from 0.02 to 0.25. Fig.7 presents the normalized maximum deflection of the solid panels and the top and bottom face sheets of sandwich panels versus the dimensionless impulse of the core. From the figure, it can be seen that, with the increase of the impulse load, the maximum deflection of the solid plate will linear increase approximatively, however, the maximum deflection of the sandwich plate will nonlinear increase. The maximum deflection of the sandwich plate less than solid plate at the same loading condition. When $\hat{I}\sqrt{\rho/\sigma_Y}/\overline{M}<0.3$, the deflection of the sandwich plate only one third of solid plate. Therefore, the Kagome truss sandwich plate is a kind of ultra-light structure with excellent impulsion resist capability.

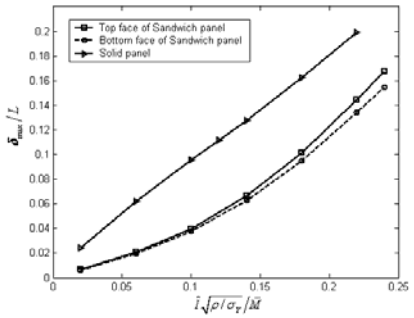

Fig.7 The normalized maximum deflection of the solid panels and the top and bottom face sheets of sandwich panels versus the dimensionless impulse of the core

7 Energy absorption in sandwich plates

When the impulse applied to the solid plate and Kagome sandwich plate with the same mass, and ignored the fluid-structure interaction, the initialized kinetic energy of the solid plate attained should be

$$E_k^{solid}=\frac{1}{2}mV_0^2=\frac{m\hat{I}^2}{2\rho^2H_s^2} \tag{19}$$

For the sandwich plate, the impulse only applied to the top face sheet, and then the initialized kinetic energy of the sandwich plate attained should be

$$E_k^{sandwich}=\frac{1}{2}m_fV_f^2=\frac{m\hat{I}^2}{2\rho^2H_sH_f} \tag{20}$$

From Eqs. (18)~(20), it can be obtained the ratio of the kinetic energy is

$$\eta=\frac{E_k^{sandwich}}{E_k^{solid}}=\frac{H_s}{H_f}=\left(2+\overline{\rho}_c\frac{H_c}{H_f}\right) \tag{21}$$

From this expression, because $H_c/H_f>0$, so that $\eta>2$. This means the energy absorbed by sandwich more than duplation by solid plate. For the optimized parameter, $\overline{\rho}_c=0.1$, $H_s/L=0.03$, $H_c/L=0.1$, from Eq. (18), it can be obtained $H_c/H_f=10$, and $\eta=3$, means the energy absorbed by sandwich will be triplication by solid plate.

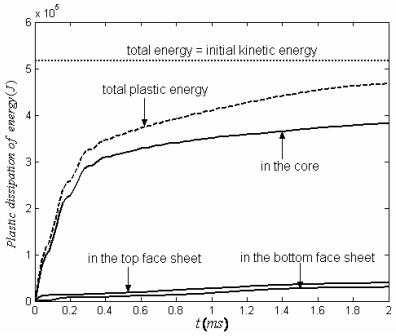

Fig.8 The time histories of plastic deformation energy in the face sheets and core of the sandwich panel

Significantly larger energy absorption in the sandwich plate relative to the corresponding solid plate can be attributed to several factors that are revealed by the time histories of plastic dissipation in the face sheets and core of the sandwich plate in Fig. 8. The time histories are for the plate with $\overline{\rho}_c=0.1$, $H_c/L=0.1$ and $\hat{I}\sqrt{\rho/\sigma_Y}/\overline{M}<0.15$. In the first phase of the response, lasting until $t\approx 0.2ms$, the top face sheet flies into the core, resulting in core compaction and significant energy dissipation. By the end of the first phase, the two face sheets are moving at approximately the same velocity and most core compaction ceases. As the plate deflection increases, plastic dissipation is increasingly due to stretch. Further details are discussed below.

Core compression constitutes a major contribution to energy dissipation. Although the crushing strength of the core is only a small fraction of σ_Y, the average compaction strain is between 10% and 20%. In the stretching phase of the response, Fig. 8 indicates there is additional plastic dissipation of energy in the core due to in-plane

stretch, although this is only a small fraction of the dissipation during crushing.

After the compaction phase has ended and as long as deflections, δ, are still less than about the sandwich thickness, H_c, the response of the sandwich plate is dominated by bending. The top face sheet experiences in-plane compression while the bottom face undergoes in-plane tension. As even larger deflections develop, stretching takes over and the in-plane stresses become tensile in both faces. Thus, the top face sheet undergoes reversed plastic deformation with compressive straining followed by tensile straining resulting in enhanced energy absorption. The solid plate undergoes a similar transition from bending to stretching but at much smaller deflections that are on the order of H_s. No plastic deformation on the top surface of the solid plate occurs during the bending phase of the corresponding solid plates. Moreover, in the bending regime, the bending strength of the sandwich plate far exceeds that of the solid plate.

8 Concluding remarks

The effective performance of 3D-Kagome truss core and the analytical model of 3D-Kagome truss core panels subjected to idealized impulsive loads is established. The transient dynamics analysis software MSC. Dytran is adopted to simulate the response of 3D-Kagome truss core panels subjected to idealized impulsive loads. Significantly impulsion resist potential of Kagome truss core sandwich can be obtained. With the increase of the proportion of the core, the stiffness and the capability for impulsion resist of the sandwich structure will increase. The Kagome truss core sandwich structure can absorb more energy than solid structure and the core compression constitutes a major contribution to energy dissipation. In a word, 3-D Kagome sandwich structure is a new kind of ultra-light structure with excellent stiffness, impulsion resist capability and energy absorption and dissipation.

The present work investigated the dynamic response of the Kagome sandwich plate under ideal impulse load and ignored the fluid-structure interaction. More work is required to assess effects of fluid-structure interaction and real loading conditions.

Acknowledgements

The present work was supported by the Major State Basic Research Development Program of China (973 Program) under grant No. 2006CB601206.

References

[1] Gibson LJ, Ashby MF. *Cellular Solids: Structure and Properties*, 2nd Edition, Cambridge University Press, Cambridge, UK, 1997.

[2] Evans AG, Hutchinson JW, Fleck NA, Ashby MF, Wadley HNG. The topological design of multifunctional cellular metals. *Progress in Materials Science*, Vol. 46, pp 309–327, 2001.

[3] Ashby MF, Evans AG, Fleck NA, Gibson LJ, Hutchinson JW, Wadley HNG. *Metal Foams: A Design Guide*, Butterworth-Heinemann, London, 2000.

[4] Wallach JC, Gibson LJ. Mechanical behavior of a three-dimensional truss material. *International Journal of Solids and Structures*, Vol. 38, pp 7181–7196, 2001.

[5] Wicks N, Hutchinson JW. Optimal truss plates. *International Journal of Solids and Structures*, Vol. 38, pp 5165–5183, 2001.

[6] Xue Z, Hutchinson JW. Preliminary assessment of sandwich plates subject to blast loads. *International Journal of Mechanical Sciences*, Vol. 45, pp 685-705, 2003.

[7] Xue Z. Hutchinson JW. A comparative study of impulse-resistant metal sandwich plates. International Journal of Impact Engineering, Vol. 30, pp 1283-1305, 2004.

[8] Wang J, Evans AG, Dharmasena K, Wadley HNG. On the performance of truss panels with Kagome cores. *International Journal of Solids and Structures*, Vol. 40, pp 6981-6988, 2003.

[9] Hyun S, Karlsson AM, Torquato S, Evans AG. Simulated properties of Kagome and tetragonal truss core panels. *International Journal of Solids and Structures*, Vol. 40, pp 6989-6998, 2003.

[10] MSC.Dytran User's Manual. Version 4.7 MSC Software Corporation. 1999.

[11] Deshpanda VS, Fleck NA. Isotropic constitutive models for metallic foams. *Journal of the Mechanics and Physics of Solids*, Vol. 48, pp 1253-83, 2000

[12] Fleck NA, Deshpande VS. The resistance of clamped sandwich beam to shock loading. Journal of Applied Mechanics. Vol. 71, pp 386-401, 2004.